Am J Cancer Res 2022;12(1):91-107
www.ajcr.us /ISSN:2156-6976/ajcr0138173

Original Article

USP47 stabilizes BACH1 to promote the Warburg effect and non-small cell lung cancer development via stimulating Hk2 and Gapdh transcription

Jing Peng, Wencan Li, Nianxi Tan, Xihua Lai, Weilin Jiang, Guang Chen

Department of Cardiothoracic Surgery, Zhuzou Central Hospital, Zhuzhou 412007, Hunan Province, China

Received August 10, 2021; Accepted December 9, 2021; Epub January 15, 2022; Published January 30, 2022

Abstract: Increasing studies demonstrated that ubiquitination plays a crucial part in the pathogenesis of non-small cell lung cancer (NSCLC), and targeted adjustment of the deubiquitination enzymes is a potential means for cancer treatment. However, the role of ubiquitin carboxyl-terminal hydrolase 47 (USP47) in NSCLC is still unclear. Here, we show that USP47 was upregulated in NSCLC clinical tissues and greatly related to advanced tumor stages and survival rate. Functional experimental results showed that USP47 promoted the cell proliferation *in vitro* and tumor growth *in vivo*. And the overexpression of USP47 promoted the glycolysis capacity of lung cancer cells. Mechanistic investigations showed that USP47 promoted NSCLC development, which depends a lot on directly binding to and deubiquitination of the basic leucine zipper transcription factor 1 (BACH1, BTB and CNC homology 1). BACH1 was also significantly overexpressed in primary NSCLC tissues and positively correlated with the expression of USP47. The promotion of USP47 on the Warburg effect and NSCLC progression was mediated by the deubiquitination of BACH1 and the downstream transcriptional regulation of hexokinase 2 (Hk2) and glyceraldehyde-phosphate dehydrogenase (Gapdh). Therefore, targeting USP47/BACH1 axis might offer a new way to inhibit the progression of NSCLC.

Keywords: Non-small cell lung cancer, USP47, BACH1, deubiquitination, Warburg effect

Introduction

With millions of confirmed cases and deaths each year, lung cancer is the leading cause of cancer-related deaths globally [1]. As the main subtype of lung cancer, non-small cell lung cancer (NSCLC) accounts for 85% of lung cancer [2]. Despite progress in diagnosis and treatment of NSCLC over decades, local recurrence, drug resistance, and metastasis are still challenges for patient prognosis, the 5 year overall survival of which only hovers around 15% [3, 4]. The exploration of NSCLC pathogenesis and the discovery of new effective therapeutic targets are both urgently needed.

In contrast with normal body cells with the respiration of oxygen, cancer cells meet their energy needs greatly through aerobic fermentation even in the presence of oxygen. These tumor features, such as increased glucose uptake, glycogen synthesis and lactate secretion, were then termed as Warburg effect [5, 6]. For example, PGC1α, peroxisome proliferator-activated receptor-gamma coactivator-1α, was recently reported to control the axis of WNT/β-catenin/pyruvate dehydrogenase kinase isozyme 1 (PDK1), inhibit aerobic glycolysis and suppress hepatocellular carcinoma metastasis [7]. In lung cancer, histone H2B monoubiquitination (H2Bub1) suppresses the Warburg effect and tumorigenesis largely via regulating multiple mitochondrial respiratory genes in human lung cancer cells [8]. In addition, hotspot mutations of isocitrate dehydrogenase 2 (IDH2) activated hypoxia-inducible factor-1α (HIF1α) pathway, thereby promoting the Warburg effect and NSCLC cell proliferation [9]. However, the mechanism of aerobic glycolysis in NSCLC still needs to be further elucidated.

Deubiquitinases were identified as specialized enzymes to counteract the ubiquitination cascade, which manipulating the ubiquitin-protea-

some system during tumorigenesis and metastasis [10]. Among them, ubiquitin carboxyl-terminal hydrolase 47 (USP47) was demonstrated as a deubiquitinase enzyme, which could counteract the activity of E3 ubiquitin ligases and be involved in the processes of cell growth and survival [11]. By quantitative proteomics, USP47 was indicated as one of the top up-regulated proteins, as well as potential therapeutic target for cancer progression management in breast cancer [12]. In colorectal cancer (CRC), USP47 served as a deubiquitinase for YAP, leading to YAP's stabilization and the aggressiveness of CRC [13]. Recognized as a novel master regulator of tumor-related genes, such as CXCR4 and MMP1, BACH1 (basic leucine zipper transcription factor 1) functions as a critical node in bone metastasis of breast cancer [14]. As yet, our understanding of USP47's role and its regulatory mechanism with BACH1 is still unclear in NSCLC.

In the present study, the USP47 expression in NSCLC tissues and its effects on cellular proliferation and tumor growth were explored. The influence of USP47 on Warburg effect was systematically studied through respectively testing lactate production, lactic dehydrogenase (LDH) activity, relative ATP content, relative glucose consumption, extracellular acidification rate (ECAR) and oxygen consumption rate (OCR). In addition, BACH1 expression and its association with USP47 in patient tissues were analyzed. Furthermore, USP47-mediated stabilization of BACH1 via deubiquitination, transcriptional activation of hexokinase 2 (Hk2) and glyceraldehyde-phosphate dehydrogenase (Gapdh) and Warburg effect were systematically researched at the molecular level. Targeting USP47/BACH1 axis might offer a new way to inhibit the progression of NSCLC.

Materials and methods

Patient tissue samples

Paired NSCLC tissue (tumor) and normal adjacent tissue (normal) samples were gathered at Zhuzhou Central Hospital. No preoperative chemotherapy or radiotherapy was administered in patients who underwent surgery. Written informed consent was acquired from each patient. Histological analysis was carried out independently by three pathologists. These experiments were performed with the permission of the Zhuzhou Central Hospital.

RNA extraction, microarray analysis and quantitative real-time PCR (qRT-PCR)

Total RNA was generated using TRIzol reagent (Thermo Fisher Scientific, Rockford, IL, USA) and then was quantified by agarose electrophoresis. The cDNA was synthesized employing the PrimeScript RT Reagent kit (Takara, Shiga, Japan). qRT-PCR was performed using SYBR Premix Ex Taq (Takara) with a 7500 detection system (Thermo Fisher Scientific). β-actin was used as the internal reference gene and the relative mRNA levels were calculated based on Equation $2^{-\Delta\Delta CT}$. The primer sequences are shown in Table S1.

Western blot

Western blot was carried out as described previously [15]. Proteins were isolated from NSCLC tissue specimens and cells with RIPA lysis buffer (Sigma-Aldrich). Protein content was measured with a BCA protein assay kit (Thermo Fisher Scientific). Using sodium dodecyl sulfate-polyacrylamide gel electrophoresis (SDS-PAGE) protein lysates were separated and then transferred to PVDF membranes (Millipore, Bedford, MA, USA). After blocking the membranes with TBST including 5% milk, the primary antibodies were incubated overnight at 4°C; afterwards, they were incubated with horseradish peroxidase-conjugated secondary antibodies and visualized using an enhanced chemiluminescence kit (Santa Cruz, Dallas, TX, USA). Protein bands were quantified with Quantity One software (Bio-Rad, Berkeley, CA, USA) using β-actin as an internal reference. Antibody information is shown in Table S2.

Immunohistochemistry (IHC) assay

Tissues were first fixed in 4% paraformaldehyde, embedded in paraffin, and then sectioned (5 μm). Antigen repair was first performed using citrate solution (95°C), and tissue sections were subjected to incubation with antibodies against USP47, Ki67 and BACH1 overnight at 4°C. To observe the expression of the target proteins, tissue sections were incubated with the corresponding secondary antibodies and visualized with 3,3'-diaminobenzidine (DAB) solution (Sigma-Aldrich, St. Louis, MO,

USA). IHC images were captured with a microscope (TE2000-U, Nikon, Japan).

Overall survival analysis

After immunohistochemical analysis, the average level of USP47 was calculated and used as a criterion to evaluate USP47 expression. When the USP47 level was higher than the average, it was categorized as "USP47 high". If the USP47 level was lower than the average, it was classified as "USP47 low". The Kaplan-Meier method was used to determine the overall survival curves of the patients according to their follow-up data.

Cell culture

Human normal lung epithelial cells (BEAS-2B) were purchased from Shanghai Institutes for Biological Sciences, Chinese Academy of Sciences (Shanghai, China). A subset of non-small cell lung cancer cell lines (CALU3, SKMES1, NCI-H520, NCI-H1573, A549, NCI-H1299) were acquired from the China National Cell Line Resource Infrastructure (Beijing, China). For BEAS-2B cells culture, LHC-9 medium was used. CALU3 and SKMES1 cells were cultured in MEM medium and RPMI-1640 medium was used for NCI-H520, NCI-H1299, NCI-H1573 and A549 cells. Cells were cultured in medium supplemented with 10% fetal bovine serum (Thermo Fisher Scientific) and stored at 37°C in a humidified environment with 5% CO_2.

Cell infection and cell transfection

The adenovirus expressing USP47 (Ad-USP47) and the adenovirus expressing USP47 shRNA (Ad-shUSP47 #1, #2, #3) and their appropriate controls (Ad-NC or Ad-shNC) were purchased from GenePharma, Shanghai, China. After infecting these adenovirus with SKMES1/CALU3 or A549/NCI-H1299 cells, adenovirus-infected cells were screened using puromycin (300 μg/mL, Sigma-Aldrich) to obtain individual clones. In addition, cells were transfected with Lipofectamine 2000 (Invitrogen), referring to the manufacturer's instructions. Ad-USP47 SKMES1 cells were transfected with shRNA for BACH1 (shBACH1) and the corresponding control (shControl). Ad-shUSP47 #1 A549 or NCI-H1299 cells were transfected with BACH1 expressing plasmid (BACH1) and the relative control (mock). The shRNAs of BACH1 and USP47 were chemically synthesized and their sequences are listed in Table S3. The BACH1 expression plasmids were constructed by enzymatic cleavage and ligation and confirmed by DNA sequencing (GenePharma) and the primer sequences are listed in Table S4.

Cell viability assay

CCK-8 cell proliferation kit (Beyotime, Shanghai, China) was used, and the instructions were referred to for cell viability assessment. Main steps: Cells were first inoculated in 96-well plates (5×10^3/well) and cultured with CCK-8 solution (10 μL, 37°C for 2 h). Then, the absorbance at 450 nm was measured by a spectrometer (Olympus, Tokyo, Japan).

Colony formation assay

SKMES1/CALU3 cells (Ad-NC or Ad-USP47) or A549/NCI-H1299 cells (Ad-shNC, Ad-shUSP-47 #1 or Ad-shUSP47 #1+BACH1) were inoculated in 6-well plates (1×10^3 cells/well) and cultured at 37°C for 2 weeks. When the cell colonies were fixed, they were stained using crystalline violet (Solarbio, Beijing, China). Finally, colonies were photographed and counted using an inverted microscope (Olympus).

Mouse xenograft model

Conduct animal experiments in accordance with the Guide for the Care and Use of Laboratory Animals published by the National Institutes of Health [16] and approved by the Ethics Committee of Zhuzou Central Hospital. The mice used for animal experiments were thymic BALB/c nude mice (16-18 g). NSCLC xenograft models were established by subcutaneous injection of SKMES1 cells (Ad-NC or Ad-USP47) and A549 cells (Ad-shNC or Ad-shUSP47 #1) into mice (6/group). Tumor volumes were measured every 3 days starting from day 7, and mice were executed on day 31 after implantation, and tumors were excised and weighed. The tumor tissues of mice were taken, and the protein expression was analyzed by immunohistochemistry for USP47 and Ki67 in the tissues, respectively.

Measurement of lactate production and lactic dehydrogenase (LDH) activity

Cells were cultured for 24 h or 48 h (5000 cells/well) in 96-well plates, and 10 mL of diluted supernatant was used to measure the lac-

tate production and LDH activity. Lactate production was determined by a Lactate Assay Kit (Sigma-Aldrich). Specifically, a master reaction mixture, consisting primarily of lactate assay buffer, lactase mixture and lactate probe, was added to each well. After mixing, the plate was incubated without light for 30 min. After that, the absorbance at 570 nm was measured and normalized to the concentration of cell protein lysates. For the measurement of LDH activity, a LDH Assay Kit (Beyotime Biotechnology, Shanghai, China) was used. Under the action of LDH, NAD^+ was reduced to NADH. Diaphorase was used to catalyze NADH and INT (2-p-nadophenyl-3-nitrophenyl tetrazolium chloride) to NAD^+ and strong chromophobe dirty (formazan). Then, the absorbance at 490 nm was determined to quantify the LDH activity.

Measurement of ATP content and glucose consumption

Cells need to be cultured for 24 h before measuring ATP content and glucose consumption. The ATP content was determined by referring to the ATP assay kit (Beyotime Biotechnology), based on the principle that firefly luciferase can catalyze the production of luciferin using the energy of ATP. When both luciferase and luciferin are in excess, the fluorescence yield is proportional to the ATP concentration over a range of concentrations. After incubating the cell lysate with ATP assay solution, the fluorescence intensity can be measured photometrically, which provides a sensitive reflection of the ATP content. Glucose consumption was measured using (Sigma-Aldrich) glucose assay kit with reference. Reagent blanks (water), standards (water + glucose standards) and test items (samples) were prepared according to the manufacturer's instructions. After adding the detection reagent, the reaction was incubated at 37°C for 30 min and terminated by adding H_2SO_4. Then, the absorbance at 540 nm was measured, and the glucose consumption was calculated by subtracting the original glucose concentration from the glucose concentration measured in the medium.

Measurement of extracellular acidification rate (ECAR) and oxygen consumption rate (OCR)

To assay ECAR, cells were cultured with unbuffered RPMI 1640 under basal conditions followed by sequential addition of glucose, mitochondrial toxin (oligomycin, Sigma-Aldrich) and glycolysis inhibitor (2-deoxyglucose, Sigma-Aldrich). To detect OCR, oligomycin, fluorophenyl cyanophenylhydrazone (FCCP), antimycin A, and rotenone (Sigma-Aldrich) were added sequentially under basal cell culture conditions. Then, ECAR and OCR were measured in non-small cell lung cancer cells utilizing a Seahorse XF96 flux analyzer (Seahorse Bioscience, Billerica, Massachusetts, USA). Both ECAR and OCR values were finally normalized to the concentration of the cellular protein lysate.

Immunofluorescence

A549 and SKMES1 cells were plated on poly-D-lysine-coated glass slides, fixed in 4% paraformaldehyde and permeabilized with 0.1% Triton X-100. Nonspecific binding was prevented by incubation with 5% BSA for 1 hour. Staining was carried out by incubating cells with anti-BACH1 and anti-USP47 antibodies overnight. The corresponding TRITC-labeled rabbit anti-goat secondary antibody and FITC-labeled goat anti-mouse/rat antibody were applied at room temperature for 1 hour, and then nuclear DAPI staining was performed. All fluorescence images were captured on a Nikon confocal microscope (C2+, Nikon, Tokyo, Japan).

Co-immunoprecipitation (Co-IP)

The USP47 expression plasmid with HA tagging and the BACH1 expression plasmid with Flag tagging were first cotransfected into HEK293T cells. Cell lysates were then prepared using IP lysis buffer (Beyotime Biotechnology) and protease inhibitor (Beyotime Biotechnology) for Co-IP experiments with HA or Flag antibodies. To reduce non-specific protein intercalation, protein lysates were incubated with 30 μL of protein A/G immunoprecipitated magnetic beads (Millipore, Massachusetts, USA). After removal of the magnetic beads, primary antibody (HA or Flag) or isotype IgG was added to the supernatant overnight at 4°C. Then, 40 μL of protein A/G beads were added to the immunoprecipitation mixture and incubated for 4 h. Protein immunoprecipitates were collected with a magnetic separator and washed 3 times using cooled IP lysis buffer. After removal of the lysis buffer, the obtained protein samples were subjected to western blot analysis. In addition, the Co-IP assay included: shUSP47 or shNC transfection of SKMES1 and

A549 cells and treatment of cells with or without MG132 (10 mM, 6 h), respectively. The prepared cell lysates were subjected to protein immunoprecipitation experiments with BACH1 antibody, and finally BACH1 ubiquitination was analyzed by immunoblotting with Poly-ub antibody.

Luciferase assay

Luciferase assay was performed as previously reported [17]. The pGL3 luciferase reporter vector (Promega, Madison, WI, USA) that contains the Gapdh or Hk2 promoter sequence and has a BACH1 wild-type or mutant binding site was first constructed. The pGL3 basic vector (E1751, Promega) was used as a negative control for the SV40 promoter-controlled luciferase vector (E1741, Promega) as a positive control. After transfection of the luciferase reporter plasmid into HEK293 cells for 24 h, luciferase activity was determined using a dual luciferase assay system (Promega).

Statistical analysis

Each experiment was performed three times independently and contained at least three samples. The samples and animals were randomly divided into experimental and control groups. The data obeyed normal distribution and the results were expressed as mean ± standard deviation (SEM). The correlation between BACH1 and USP47 was analyzed using Pearson correlation analysis. Statistical differences between the two groups were analyzed by Student's t-test, and statistical differences between multiple groups were analyzed by one-way ANOVA. $P<0.01$ was classified as significant. $^{*}P<0.05$, $^{\#}P<0.05$; $^{**}P<0.01$, $^{\#\#}P<0.01$.

Results

USP47 is up-regulated in NSCLC tissues

To investigate the expression of USP47 in NSCLC, qRT-PCR was used to detect the levels of USP47 in NSCLC tissues (tumor, n=87) and normal paracancerous tissues (normal, n=87). USP47 was remarkably upregulated in NSCLC tissues (**Figure 1A**). USP47 mRNA level of patients in III-IV phases was higher than that of patients in I-II phases. However, there is no significant difference in the expression of USP47 between metastatic and non-metastatic patients, suggesting that USP47 may largely affected the growth process of NSCLC. As is shown in **Figure 1B**, western blot results showed that USP47 protein expression was elevated in the tumor tissues of NSCLC patients. In addition, IHC results further confirmed that USP47 was highly expressed in NSCLC tissues, and the intensity of USP47 immunostaining was higher in stage III patients than in stage I patients (**Figure 1C**). The results of Kaplan-Meier analysis showed that NSCLC patients with high USP47 expression had relatively lower survival rates (**Figure 1D**). The above results suggest that USP47 may play an important role in the pathogenesis of NSCLC.

USP47 affects NSCLC cell proliferation and tumor growth

To investigate the biological function of USP47, we first examined the expression of USP47 in human normal lung epithelial cells and non-small cell lung cancer cells such as CALU3, SKMES1, NCI-H520, NCI-H1573, A549 and NCI-H1299. As shown in **Figure 2A**, the expression level of USP47 was higher in NSCLC cells than in BEAS-2B cells. Because USP47 expression was lower in SKMES1 and CALU3 cells, and higher in A549 and NCI-H1299 cells, we selected these four cells for the follow-up study. As shown in **Figure 2B**, SKMES1 and CALU3 cells with stable overexpression of USP47 (Ad-USP47 group) and A549 and NCI-H1299 cells with stable down-regulation of USP47 (Ad-shUSP47 #1 group) were successfully constructed and validated by western blot. The control cells were Ad-NC and Ad-shNC, respectively. Ad-shUSP47 #1 interfered most significantly and was therefore chosen to interfere with USP47 expression. The viability of SKMES1 and CALU3 cells was higher in the Ad-USP47 group compared to the Ad-NC group. In contrast, cell viability showed the opposite trend after USP47 down-regulation in A549 and NCI-H1299 cells (**Figure 2C**). The results of cell colony formation assay showed that the number of colonies in SKMES1 and CALU3 cells in Ad-USP47 group was higher than that in Ad-NC group. The number of A549 and NCI-H1299 cell clones was lower in the Ad-shNC group compared to the Ad-shUSP47 #1 group (**Figure 2D**). Moreover,

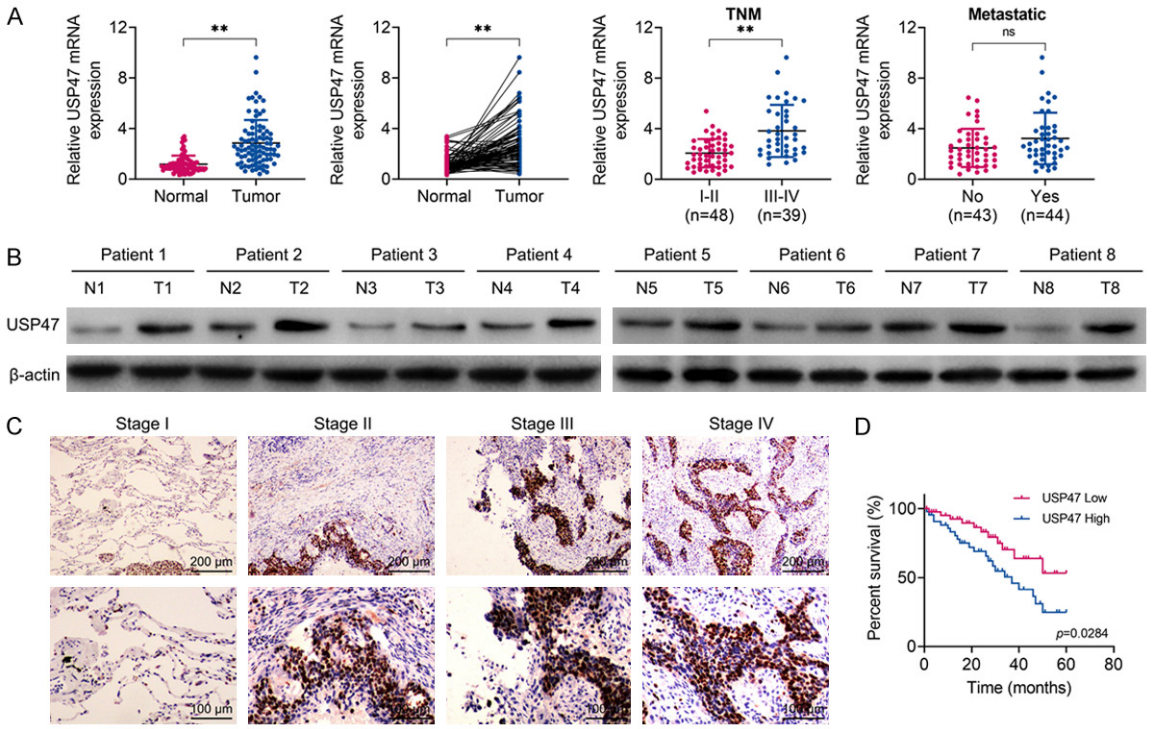

Figure 1. USP47 is upregulated in NSCLC and is associated with patient prognosis. A. Relative USP47 mRNA expression levels in NSCLC tissues (tumor, n=87) and normal adjacent tissues (normal, n=87), represented as scatter diagram and line chart (left). Relative USP47 mRNA expression levels in tumor tissues of NSCLC patients at phase I-II and III-IV, or patients with metastasis (Yes) or without metastasis (No), represented as scatter diagram (right). B. USP47 protein expression levels in NSCLC tissues (T, n=8) and normal adjacent tissues (N, n=8), as determined using western blotting. C. Representative images of USP47 IHC staining in NSCLC tissues at phage at I, II, III and IV. Original magnification, 400×. D. Kaplan-Meier curves of overall survival of 87 NSCLC patients, stratified by USP47 expression. (Mean ± SEM, **P<0.01, ns, no significance).

suppression of USP47 in USP47 overespressing SKMES1 cells could rescue stimulative-cell viability and colony formation. Accordingly, overexpression of USP47 in USP47 depletion A549 cells could rescue inhibited-cell viability and colony formation (Figure S2).

In addition, we also investigated the role of USP47 in a mouse model. A xenograft mouse model was successfully constructed by subcutaneous injection of SKMES1 cells (Ad-USP47, Ad-NC) and A549 cells (Ad-shNC, Ad-shUSP47 #1). At 31 days after cell implantation, the tumor volume of mice in the Ad-USP47 group was significantly larger than that in the Ad-NC group, and the tumor weight was significantly larger than that in the Ad-NC group. However, the tumors in the Ad-shUSP47 #1 group were smaller and lighter compared to the Ad-shNC group (**Figure 2E**). As shown in **Figure 2F**, immunohistochemical results showed that USP47 upregulation could lead to increased Ki67 expression in tumor tissues of the Ad-USP47 group; USP47 downregulation led to decreased Ki67 expression. The above results suggested that USP47 could promote NSCLC cell proliferation and tumor growth.

USP47 promotes the Warburg effect of NSCLC cells

The Warburg effect is an aerobic glycolytic phenomenon, which refers to the abnormal metabolism of cancer cells with a high degree of glycolysis, increased glucose uptake, and increased lactate production to provide the energy required for tumor growth, even in the presence of sufficient oxygen. To further understand the mechanism of action of USP47, we examined lactate production, lactate dehydrogenase (LDH) activity, ATP content, glucose consumption, extracellular acidification rate (ECAR) and oxygen consumption rate (OCR) in NSCLC cells, respectively. Up-regulation of

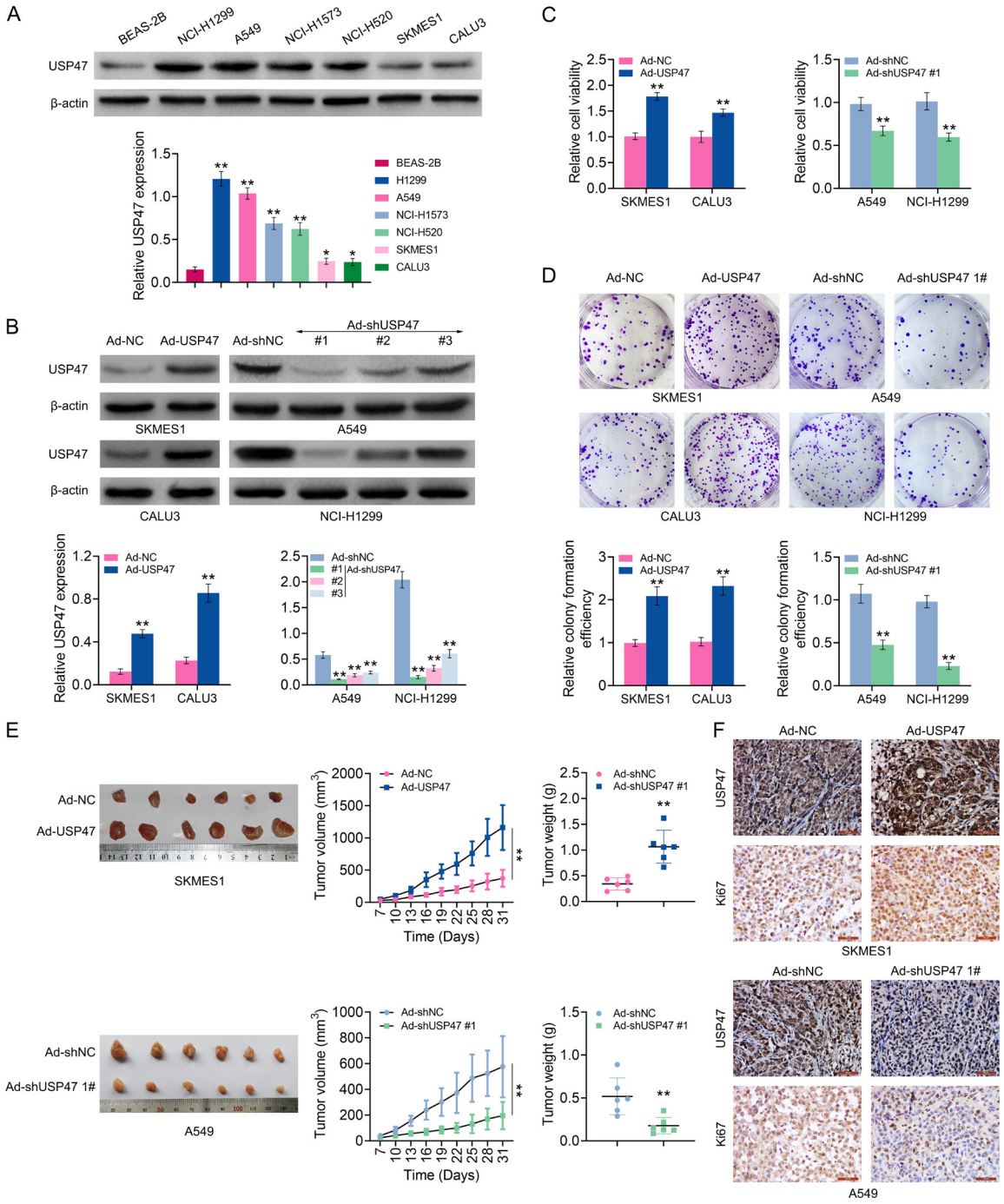

Figure 2. USP47 affects NSCLC cell proliferation and tumor growth. A. USP47 protein expression levels in human normal lung epithelial cells (BEAS-2B) and some kinds of NSCLC cells (CALU3, SKMES1, NCI-H520, NCI-H1573, A549 and NCI-H1299), as determined using western blotting. Bands were quantified and shown in histogram. B. USP47 protein expression levels in SKMES1, CALU3 cells stably overexpressing USP47 (Ad-USP47), A549 and NCI-H1299 cells stably downregulating USP47 (Ad-shUSP47 #1, #2, #3) and the control cells (Ad-NC, Ad-shNC), as determined using western blotting. Bands were quantified and shown in histogram. C. Relative cell viability of SKMES1, CALU3 cells stably overexpressing USP47 (Ad-USP47), A549 and NCI-H1299 cells stably downregulating USP47 (Ad-shUSP47 #1) and the control cells (Ad-NC, Ad-shNC). Measurements of the cell viability were obtained using a CCK-8 kit. D. Colony formation analysis of SKMES1, CALU3 cells stably overexpressing USP47 (Ad-USP47), A549 and NCI-H1299 cells stably downregulating USP47 (Ad-shUSP47 #1) and the control cells (Ad-NC, Ad-shNC). Relative colony formation efficiency was quantified. E. Image of corresponding xenograft tumors derived from subcutaneous implantation of SKMES1 cells stably overexpressing USP47 (Ad-USP47), A549 cells stably downregulating USP47 (Ad-shUSP47 #1) and the control cells (Ad-NC, Ad-shNC). Quantification of the tumor volumes and weight was shown as histograms. F. Representative images of USP47 IHC staining in the xenograft tumors. Scale bar =50 μm. (Mean ± SEM, $^{**}P<0.01$).

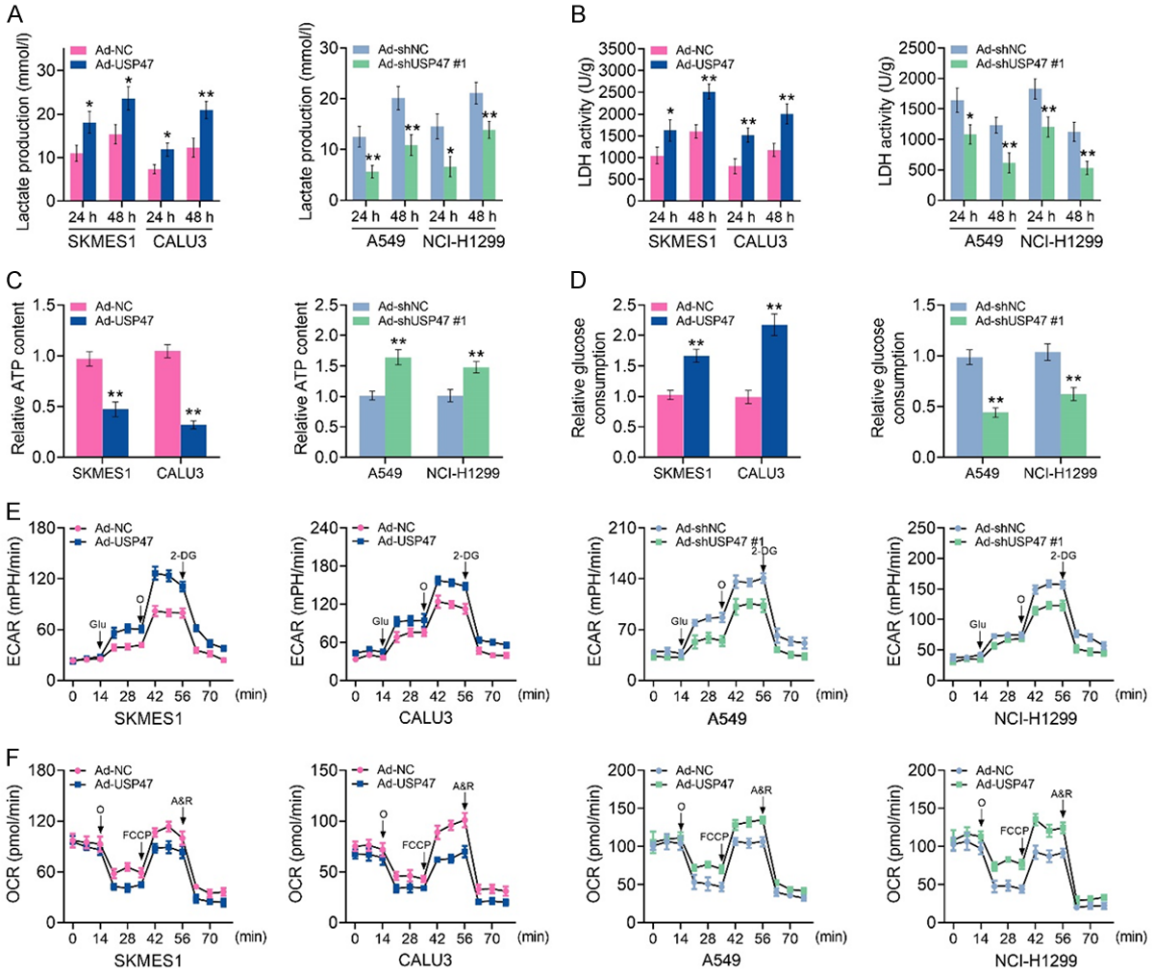

Figure 3. USP47 promotes the Warburg effect of NSCLC cells. A. Lactate production in SKMES1, CALU3 cells stably overexpressing USP47 (Ad-USP47), A549 and NCI-H1299 cells stably downregulating USP47 (Ad-shUSP47 #1) and the control cells (Ad-NC, Ad-shNC). B. Lactic dehydrogenase (LDH) in SKMES1, CALU3 cells stably overexpressing USP47 (Ad-USP47), A549 and NCI-H1299 cells stably downregulating USP47 (Ad-shUSP47 #1) and the control cells (Ad-NC, Ad-shNC). C. Relative ATP content in SKMES1, CALU3 cells stably overexpressing USP47 (Ad-USP47), A549 and NCI-H1299 cells stably downregulating USP47 (Ad-shUSP47 #1) and the control cells (Ad-NC, Ad-shNC). D. Relative glucose consumption in SKMES1, CALU3 cells stably overexpressing USP47 (Ad-USP47), A549 and NCI-H1299 cells stably downregulating USP47 (Ad-shUSP47 #1) and the control cells (Ad-NC, Ad-shNC). E. Extracellular acidification rate (ECAR) in SKMES1, CALU3 cells stably overexpressing USP47 (Ad-USP47), A549 and NCI-H1299 cells stably downregulating USP47 (Ad-shUSP47 #1) and the control cells (Ad-NC, Ad-shNC). F. Oxygen consumption rate (OCR) in SKMES1, CALU3 cells stably overexpressing USP47 (Ad-USP47), A549 and NCI-H1299 cells stably downregulating USP47 (Ad-shUSP47 #1) and the control cells (Ad-NC, Ad-shNC). (Mean ± SEM, $^{**}P<0.01$).

USP47 increased lactate production and LDH activity in SKMES1 and CALU3 cells compared to the Ad-NC group. In contrast, downregulation of USP47 resulted in decreased lactate production levels and LDH activity in A549 and H1299 cells (**Figure 3A** and **3B**). In addition, A549 and H1299 cells overexpressing USP47 (Ad-USP47) had lower ATP content and higher glucose consumption compared with normal cells (Ad-NC). Accordingly, the down-regulation of USP47 led to the opposite result (**Figure 3C** and **3D**). As shown in **Figure 3E** and **3F**, USP47 upregulation inhibited ECAR, an indicator of glycolysis, and OCR, a mitochondrial oxidative phosphorylation, in SKMES1 and CALU3 cells compared with the Ad-NC group. The ECAR and OCR in A549 and NCI-H1299 cells in the Ad-shUSP47 #1 group were significantly higher than those in the Ad-shNC group. The above results suggest that the promotion of lung cell proliferation by USP47 may be mainly dependent on the regulation of Warburg effect.

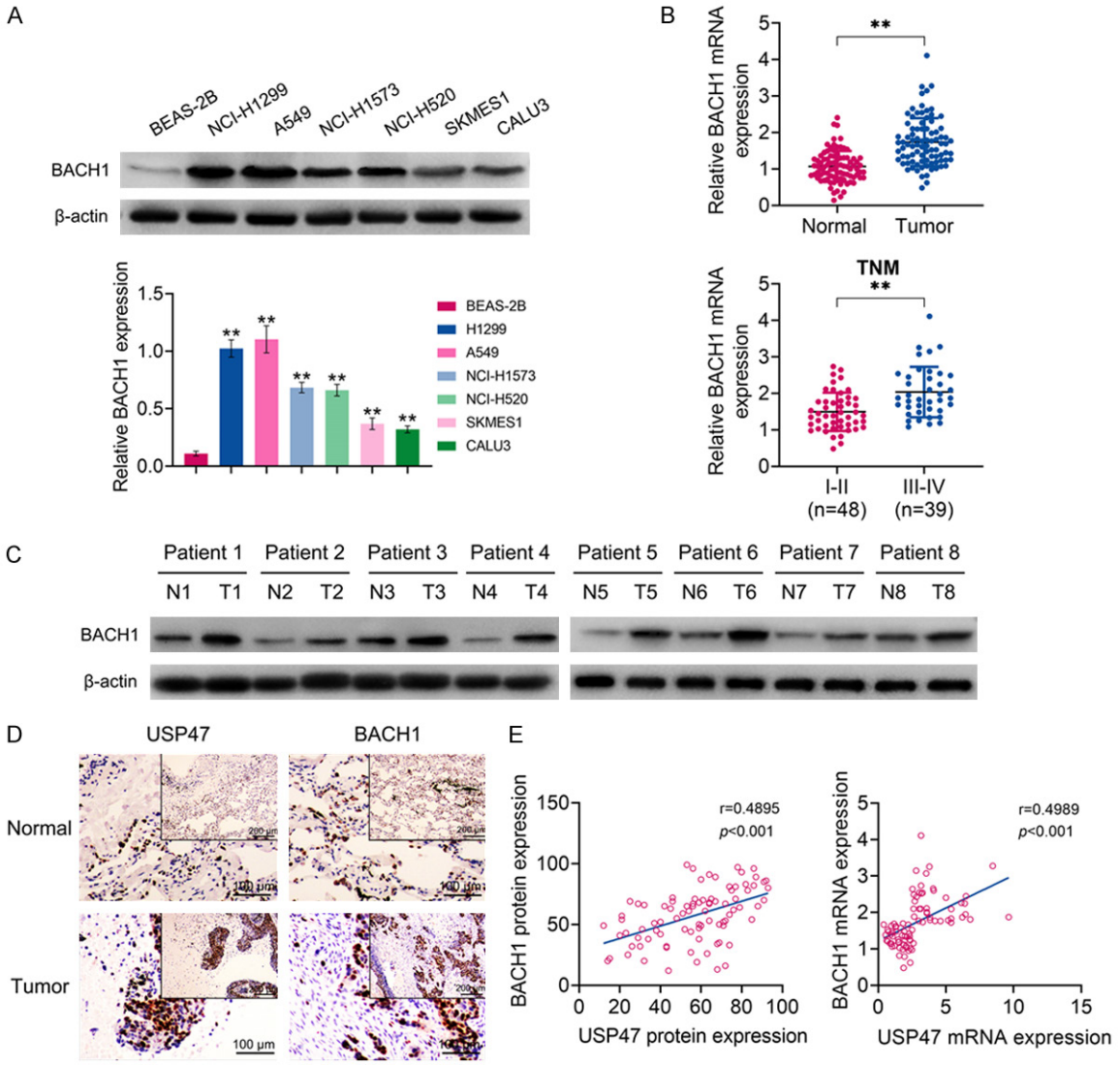

Figure 4. BACH1 is up-regulated and positively correlates with USP47 expression in NSCLC tissues. A. BACH1 protein expression levels in human normal lung epithelial cells (BEAS-2B) and some kinds of NSCLC cells (CALU3, SKMES1, NCI-H520, NCI-H1573, A549 and NCI-H1299), as determined using western blotting. Bands were quantified and shown in histogram. B. Relative BACH1 mRNA expression levels in NSCLC tissues (tumor, n=87) and normal adjacent tissues (normal, n=87, up). Relative BACH1 mRNA expression levels in tumor tissues of NSCLC patients at phase I-II and III-IV (down). C. BACH1 protein expression levels in NSCLC tissues (T, n=8) and normal adjacent tissues (N, n=8), as determined using western blotting. D. Representative images of BACH1 IHC staining in NSCLC tissues (tumor, n=87) and normal adjacent tissues (normal, n=87, up). Original magnification, 400×. E. Pearson's correlation analysis of the relative protein and mRNA expressions between USP47 and BACH1. (Mean ± SEM, $^{**}P<0.01$).

BACH1 expression is up-regulated and positively correlates with USP47 expression in NSCLC tissues

To explore BACH1's role in NSCLC, its expression in BEAS-2B cells and NSCLC cells was analyzed by western blot. The results in **Figure 4A** showed that BACH1 was remarkably upregulated in NSCLC cells compared to BEAS-2B cells. As shown in **Figure 4B**, qRT-PCR results in patient tissues showed that BACH1 mRNA level in NSCLC tissues (tumor, n=87) was higher than that in normal adjacent tissues (normal, n=87). BACH1 mRNA level of patients in III-IV phases was higher than that of patients in I-II phases. In addition, the results of western blot showed that BACH1 protein expression was increased in tumor tissues of NSCLC patients, which also were used to detect USP47 protein expression (**Figure 4C**). Moreover, the

results of IHC in **Figure 4D** showed that USP47 was highly expressed in NSCLC tissues. By means of Pearson correlation analysis, positive correlations were determined in the relative protein expression and mRNA expression between BACH1 and USP47 in clinical NSCLC tissues (**Figure 4E**). Analyses of The Cancer Genome Atlas (TCGA) database showed that USP47 and BACH1 expression were positively correlated in both lung adenocarcinoma and lung squamous carcinoma (Figure S1). Whereas, the effect of USP47 on BACH1 protein expression still needs further investigation.

USP47 interacts with and stabilizes BACH1 in NSCLC cells

To explore the effect of USP47 on BACH1 expression, we detected the expression of BACH1 mRNA and protein in non-small cell lung cancer cells by up- or down-regulating USP47. As is shown in **Figure 5A** and **5B**, after USP47 inhibition in A549 and NCI-H1299 cells, USP47 was overexpressed in SKMES1 and CALU3 cells, while BACH1 mRNA levels were not significantly changed. In contrast, upregulation of USP47 expression resulted in elevated BACH1 protein levels, whereas downregulation of USP47 expression resulted in decreased BACH1 protein levels. Moreover, immunofluorescent staining demonstrated that the fluorescences of USP47 and BACH1 highly overlapped (**Figure 5C**). Therefore, the hypothesis was proposed that USP47 can interact with BACH1 and increase BACH1 stability by deubiquitination, thus regulating lung cancer cell glucose metabolism and tumor progression.

Next, to elucidate the molecular mechanism by which USP47 promotes BACH1 protein expression, we performed protein co-immunoprecipitation experiments. First, Flag-BACH1 and HA-USP47 co-expression was achieved in HEK293 cells. BACH1 and USP47 were immunoprecipitated using Flag or HA antibodies. Then, the proteins pulled down by Flag or HA antibodies were identified by western blot. Immunoprecipitation of BACH1 using Flag antibody detected USP47 in the pull-down protein samples. Similarly, immunoprecipitation of USP47 using HA antibody detected BACH1 in the pull-down protein samples (**Figure 5D**). This suggests an endogenous interaction between USP47 and BACH1. To investigate whether the deubiquitinating enzyme USP47 regulates BACH1 ubiquitination, endogenous BACH1 expression was first examined after MG132 treatment in SKMES1 and A549 cells. The results showed that BACH1 protein expression increased accompanied by prolonged MG132 treatment (**Figure 5E**). We next examined the protein levels of Flag-BACH1 in MG132 treated or untreated HEK293, SKMES1 and A549 cells. BACH1 protein expression was significantly upregulated after MG132 treatment (**Figure 5F**). After that, we studied whether polyubiquitin modification of BACH1 protein was affected by USP47-mediated deubiquitination. Immunoprecipitation and immunoblotting analysis were performed with BACH1 and polyb antibodies. The results showed that USP47 knockdown significantly increased the level of BACH1 ubiquitination in SKMES1 and A549 cells in the presence of MG132 (**Figure 5E**). To verify whether USP47 could play a role in stabilizing BACH1 protein expression, we examined the effect of USP47 downregulation on the stability of endogenous BACH1 protein after treatment with the protein synthesis inhibitor cycloheximide (CHX). In A549 cells, the half-life of BACH1 protein was significantly reduced in USP47 knockdown cells (shUSP47) compared to control cells (shRNA) (**Figure 5F**). The above results suggest that USP47 may stabilize the expression of BACH1 in NSCLC cells through deubiquitination.

USP47 activates BACH1-mediated transcription of Hk2 and Gapdh

The above studies demonstrate that USP47 can deubiquitinate and promote the expression of BACH1 in NSCLC cells. It was previously demonstrated that BACH1 could activate Hk2 and Gapdh transcription and trigger glycolysis-induced metastasis in NSCLC [17]. To identify whether USP47 is responsible for the transcriptional activation of Hk2 and Gapdh, the expression levels of Hk2 and Gapdh were determined in NSCLC cells with upregulation or inhibition of USP47. As shown in **Figure 6A** and **6B**, both mRNA and protein expressions were higher in SKMES1, CALU3 cells stably overexpressing USP47, compared to the control cells. Accordingly, the opposite result can be obtained in A549 and NCI-H1299 cells from Ad-shUSP47 #1 group, compared to cells from Ad-shNC group. The results also showed that USP47 overexpression caused BACH1 upregulation, and USP47 downregulation led to BA-

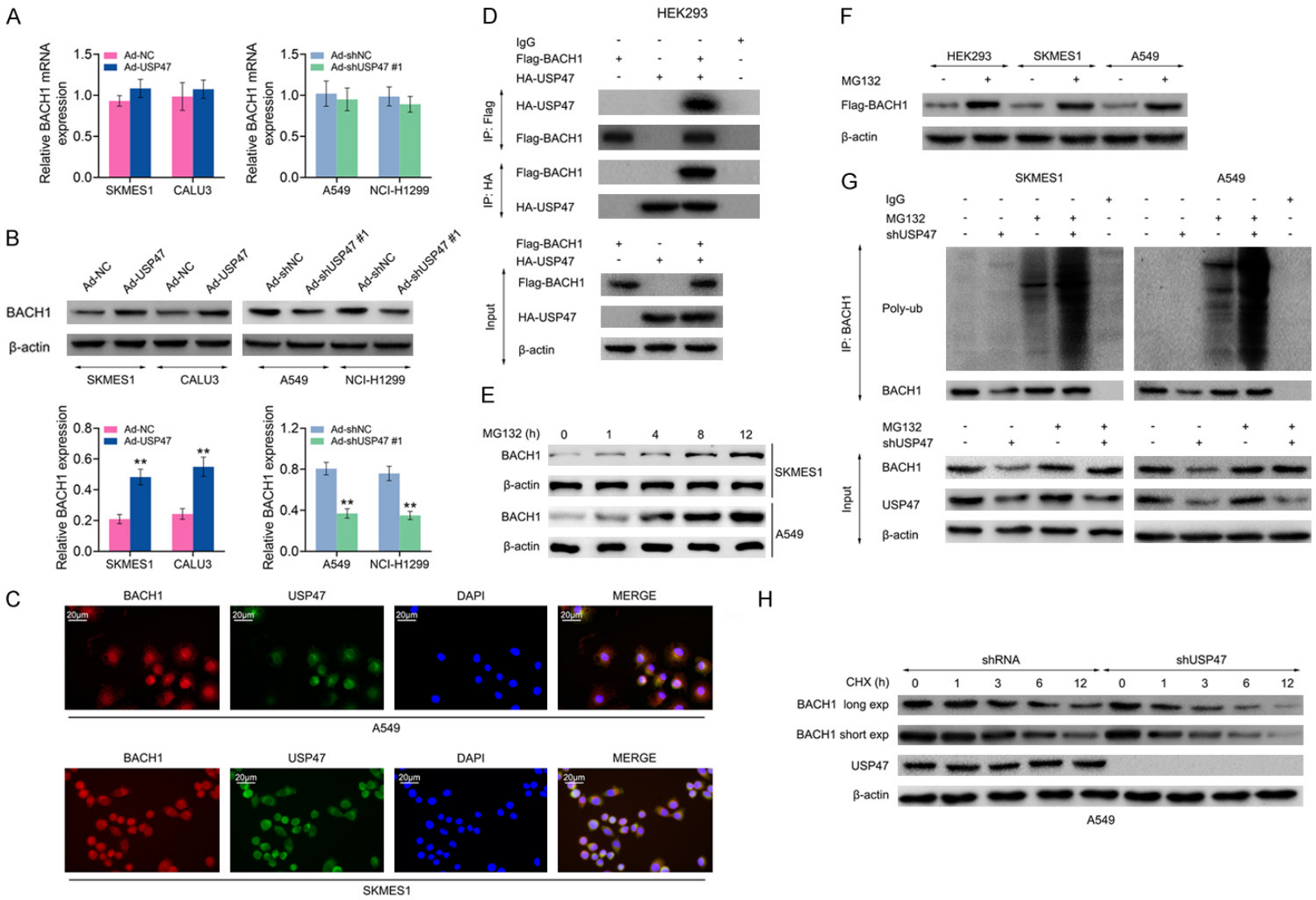

Figure 5. USP47 interacts with and stabilizes BACH1 in NSCLC cells. A. Relative BACH1 mRNA expression levels in SKMES1, CALU3 cells stably overexpressing USP47 (Ad-USP47), A549 and NCI-H1299 cells stably downregulating USP47 (Ad-shUSP47 #1) and the control cells (Ad-NC, Ad-shNC), as determined using qRT-PCR. B. BACH1 protein expression levels in SKMES1, CALU3 cells stably overexpressing USP47 (Ad-USP47), A549 and NCI-H1299 cells stably downregulating USP47 (Ad-shUSP47 #1) and the control cells (Ad-NC, Ad-shNC), as determined using western blotting. Bands were quantified and shown in histogram. C. Representa-

tive photos of immunofluorescence staining for BACH1 and USP47 (red, BACH1; green, USP47; blue, DAPI nuclear staining). Scale bar, 20 mm. D. Immunoprecipitation was carried out using anti-Flag, anti-HA or IgG antibodies, and specific associations between USP47 and BACH1 were analyzed by western blotting in HEK293 cells transfected with plasmids encoding HA-tagged USP47 and Flag-BACH1. E. BACH1 protein expression levels in SKMES1 and A549 cells with MG132 treatment at 0 h, 1 h, 4 h, 8 h and 12 h. F. BACH1 protein expression levels in HEK293, SKMES1 and A549 cells with or without MG132 treatment after transfected with plasmids encoding Flag-BACH1. G. Immunoprecipitation was carried out using anti-BACH1 or IgG antibodies, and ubiquitination levels of BACH1 were analyzed by western blotting in SKMES1 and A549 cells with USP47 downregualtion (shUSP47), with MG132 treatment (MG132) or with USP47 downregualtion & MG132 treatment (shUSP47+MG132). H. A549 cells stably downregulating USP47 (Ad-shUSP47) and the control cells (shRNA), were treated with CHX (100 μg/ml) for the indicated time points. Protein levels of BACH1 and USP47 were analyzed by western blotting. (Mean ± SEM, $^{**}P<0.01$).

CH1 suppression. Additionally, the results of qRT-PCR and western blot showed that up-regulation of Hk2 and Gapdh were significantly relowered by the down-regulation of BACH1. Conversely, BACH1 overexpression restored the downregulated-expression of Hk2 and Gapdh, which was mediated by USP47 inhibition (**Figure 6C** and **6D**). Moreover, the results in Figure S3 showed that USP47 inhibitor P22077 suppress cell viability, colony formation and protein levels of BACH1, Hk2 and Gapdh. As shown in **Figure 6E**, overexpression of USP47 upregulated the luciferase activity of the Hk2 and Gapdh promoters in HEK293 cells. However, no significant changes in luciferase activity were detected after mutating the binding sites. It can be seen that USP47 regulates glycolysis through BACH1 by activating the transcription of Hk2 and Gapdh, which in turn enables the regulation of glycolysis by USP47 through BACH1.

USP47 enhances the Warburg effect via the stabilization of BACH1

Preceding results showed that USP47 activates BACH1-mediated transcription of Hk2 and Gapdh, whether USP47 caused-Warburg effect is mediated by BACH1 was researched next. The viability and colony number of SKMES1 and A549 cells was higher in the group overexpressing BACH1 (BACH1) compared to the Mock group (Figure S4). As shown in **Figure 7A**, downregulation of USP47 expression inhibited cell viability in A549 and NCI-H1299 cells, while overexpression of BACH1 at this time restored cell viability. The results of cell colony formation indicated that downregulation of USP47 decreased the number of cell clones, and the effect caused by USP47 inhibition could be rescued by BACH1 overexpression (**Figure 7B**). In addition, USP47 downregulation had an inhibitory effect on lactate production and LDH activity in A549 and H1299 cells, which could also be restored by overexpression of BACH1 (**Figure 7C** and **7D**). Furthermore, downregulation of USP47 in A549 and H1299 cells also reduced elevated ATP content and glucose consumption. Similarly, BACH1 overexpression eliminated the changes in ATP content and glucose consumption caused by inhibition of USP47 (**Figure 7E** and **7F**).

Furthermore, ECAR and OCR analysis indicated that downregulation of USP47 suppressed the ECAR and OCR of A549 and NCI-H1299 cells from Ad-shUSP47 #1 group, which was also restored by BACH1 overexpression (**Figure 7G** and **7H**). The above results suggest that USP47 promotes the Warburg effect and ultimately the development of NSCLC by stabilizing the expression of BACH1.

Discussion

Elucidating the mechanisms of epigenetic modifications is necessary to gain insight into tumor pathogenesis and treatment, and the role and mechanisms of some important deubiquitinating enzymes in lung carcinogenesis are receiving increasing attention. For example, F-box and WD repeat domain containing 2 (FBXW2) inhibits migration and invasion of lung cancer cells by promoting the ubiquitylation and degradation of β-catenin [18]. USP37, a deubiquitinating enzyme (DUB) family member, can deubiquitinate and prevent degradation of Snail, thereby promoting lung cancer cell migration [19]. In addition, GIAT4RA, a newly identified lncRNA, was found to be essential for the degradation of chromatin modifier lymphoid-specific helicase (LSH) by counteracting ubiquitin hydrolase Uchl3-mediated interaction and stabilization of LSH in NSCLC [20]. Our results not only first showed the stimulative function of USP47 on tumor growth in NSCLC, but also identified a regulatory relationship between USP47 and BACH1. Recently, some miRNAs

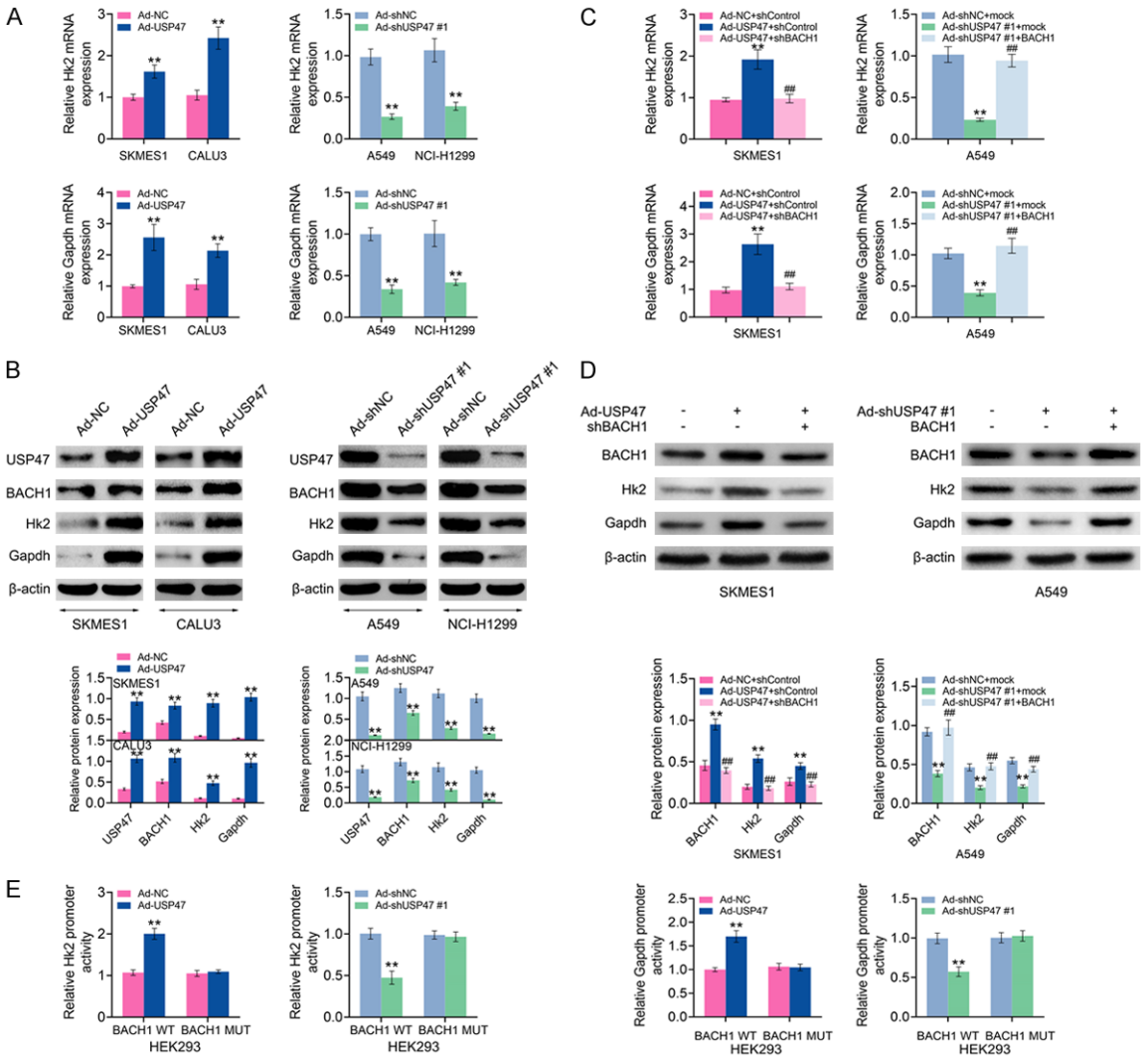

Figure 6. USP47 activates BACH1-mediated transcription of Hk2 and Gapdh. A. Relative Hk2 and Gapdh mRNA expression levels in SKMES1, CALU3 cells stably overexpressing USP47 (Ad-USP47), A549 and NCI-H1299 cells stably downregulating USP47 (Ad-shUSP47 #1) and the control cells (Ad-NC, Ad-shNC), as determined using qRT-PCR. B. USP47, BACH1, Hk2 and Gapdh protein expression levels in SKMES1, CALU3 cells stably overexpressing USP47 (Ad-USP47), A549 and NCI-H1299 cells stably downregulating USP47 (Ad-shUSP47 #1) and the control cells (Ad-NC, Ad-shNC), as determined using western blotting. Bands were quantified and shown in histogram. C. Relative Hk2 and Gapdh mRNA expression levels in SKMES1 cells stably overexpressing USP47 (Ad-USP47+shControl), stably overexpressing USP47 with BACH1 downregulation (Ad-USP47+shBACH1), and the control cells (Ad-NC+shControl). Relative Hk2 and Gapdh mRNA expression levels in A549 cells stably downregulating USP47 (Ad-shUSP47 #1+mock), stably downregulating USP47 with BACH1 upregulation (Ad-shUSP47 #1+BACH1), and the control cells (Ad-shNC+mock). D. Relative BACH1, Hk2 and Gapdh protein expression levels in SKMES1 cells stably overexpressing USP47 (Ad-USP47+shControl), stably overexpressing USP47 with BACH1 downregulation (Ad-USP47+shBACH1), and the control cells (Ad-NC+shControl). Relative Hk2 and Gapdh protein expression levels in A549 cells stably downregulating USP47 (Ad-shUSP47 #1+mock), stably downregulating USP47 with BACH1 upregulation (Ad-shUSP47 #1+BACH1), and the control cells (Ad-shNC+mock). Bands were quantified and shown in histogram. E. Relative luciferase activity of the pGL3 luciferase reporter vector containing BACH1 promoter sequences with BACH1 motifs or mutated motifs in HEK293 cells stably overexpressing USP47 (Ad-USP47), stably downregulating USP47 (Ad-shUSP47 #1) and the control cells (Ad-NC, Ad-shNC). (Mean ± SEM, $^{**}P<0.01$, $^{\#\#}P<0.01$).

were reported to target USP47 in tumors, among which are miR-204-5p in gastric cancer and ovarian cancer, and miR-188-5p in colorectal cancer [21-23]. So far, only miR-204-5p was demonstrated to be down-regulated in lung cancer. Whether miR-204-5p and other miR-

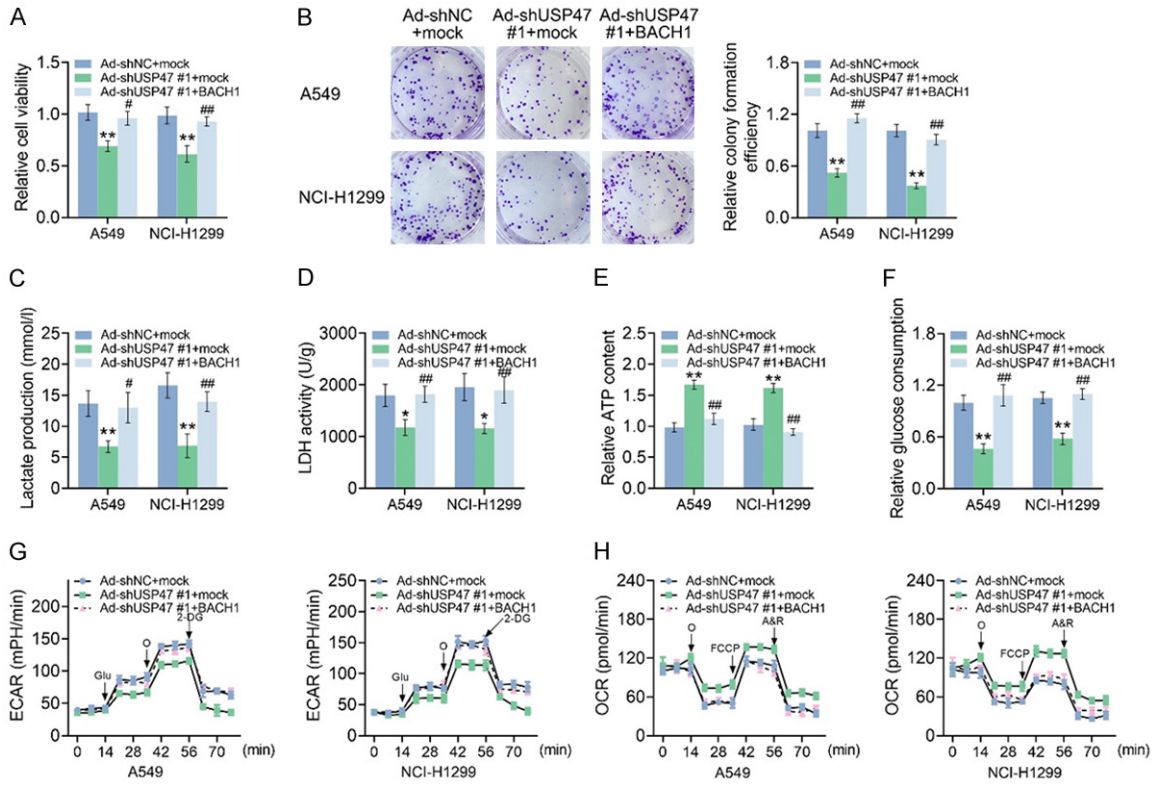

Figure 7. USP47 enhances the Warburg effect via the stabilization of BACH1. (A) Relative cell viability of A549 cells stably downregulating USP47 (Ad-shUSP47 #1+mock), stably downregulating USP47 with BACH1 upregulation (Ad-shUSP47 #1+BACH1), and the control cells (Ad-shNC+mock). Measurements of the cell viability were obtained using a CCK-8 kit. (B) Colony formation analysis of A549 cells stably downregulating USP47 (Ad-shUSP47 #1+mock), stably downregulating USP47 with BACH1 upregulation (Ad-shUSP47 #1+BACH1), and the control cells (Ad-shNC+mock). Relative colony formation efficiency was quantified. (C) Lactate production and (D) Lactic dehydrogenase (LDH) in A549 cells stably downregulating USP47 (Ad-shUSP47 #1+mock), stably downregulating USP47 with BACH1 upregulation (Ad-shUSP47 #1+BACH1), and the control cells (Ad-shNC+mock). (E) Relative ATP content and (F) Relative glucose consumption in A549 cells stably downregulating USP47 (Ad-shUSP47 #1+mock), stably downregulating USP47 with BACH1 upregulation (Ad-shUSP47 #1+BACH1), and the control cells (Ad-shNC+mock). (G) Extracellular acidification rate (ECAR) and (H) Oxygen consumption rate (OCR) in A549 cells stably downregulating USP47 (Ad-shUSP47 #1+mock), stably downregulating USP47 with BACH1 upregulation (Ad-shUSP47 #1+BACH1), and the control cells (Ad-shNC+mock). (Mean ± SEM, $^{*}P<0.05$, $^{\#}P<0.05$; $^{**}P<0.01$, $^{\#\#}P<0.01$).

NAs are responsible for the upregulation of USP47 deserves further study [24].

This study reveals that USP47 plays a key regulatory role in the Warburg effect by inhibiting the ubiquitination of BACH1. Recent studies have reported that in NSCLC, heme and F-box protein Fbx22 (FBXO22)-mediated degradation of BACH1 can be inhibited by Nrf2 (Nfe2l2 gene product) protein, suggesting that inhibition of Nrf2 and its mediated signaling might inhibit the development of NSCLC [25]. In addition, antioxidants, such as n-acetylcysteine and vitamin E, stabilize the protein expression of transcription factor BACH1, upregulate the transcript levels of hexokinase 2 and Gapdh, and increase glucose uptake and lactate secretion in tumor cells, thereby accelerating the distal metastatic process of lung cancer cells [17]. In the present study, we found that USP47 also stabilized BACH1, and overexpression of BACH1 had a restorative effect on cell proliferation inhibition and aerobic glycolysis mediated by USP47 downregulation (Figure S5). In addition to BACH1, USP47 also promoted the stability of gastric cancer β-transduced repeat-containing protein (βTrCP) protein, suggesting that downregulation of USP47 may be a way to inhibit gastric cancer cell survival and improve chemotherapy resistance [26]. In addition, it has also been shown that USP47 promotes the deubiquitination of specific AT-rich sequence bind-

ing protein-1 (SATB1) in colon cancer and improves the protein stability of SATB1 [27]. The above studies provide evidence that USP47 is associated with the regulation of ubiquitination and an idea to treat tumors by regulating the expression of deubiquitinating enzymes (e.g., USP47).

As a key regulator of many genes, the ubiquitin system directly or indirectly regulates cell signaling and strictly controls physiopathological processes [28]. Based on the fact that the expression changes or activity abnormalities of deubiquitinating enzymes are associated with tumor development, highly effective inhibitors of them are expected to be promising for treatment in multiple malignancies in addition to NSCLC [29]. At present, the anti-tumor effects of some small molecule inhibitors of deubiquitinating enzymes have been demonstrated. For example, WP1130 can inhibit the activity of deubiquitination enzymes USP9X, USP5, USP14 and UCH37, down-regulate anti-apoptotic protein MCL-1 and up-regulate tumor suppressor p53 to improve the anti-tumor therapy [30]. Recent study showed that WP1130 could increase cisplatin sensitivity by inhibiting ubiquitin-specific peptidase 9, X-linked (usp9x) in estrogen receptor-negative breast cancer cells [31]. As the first proteasome inhibitor approved by the FDA for multiple myeloma treatment, Bortezomib (PS-341) showed an active therapeutic activity in a variety of NSCLC animal models [32]. However, Inadequate efficacy of erlotinib in combination with bortezomib can be seen in patients with relapsed/refractory advanced NSCLC [33]. Based on the elucidation of drug regulatory mechanisms and their effects on signal transduction, the design of specific and effective deubiquitination inhibitors or activators, or their combination with conventional antitumor drugs may improve the treatment status and bring benefits to patients. In summary, USP47 was over-expressed in NSCLC clinical tissues and positively correlated with the expression of BACH1. Cell proliferation and tumor growth was inhibited by USP47 downregulation in NSCLC cells. In addition, USP47 overexpression enhanced the Warburg effect in NSCLC cells, which was involved in the interaction and stabilization of BACH1. Our findings provide a new option to inhibit the progression of non-small cell lung cancer by targeting the USP47/BACH1 axis.

Acknowledgements

Written informed consent was obtained from a legally authorized representative(s) for anonymized patient information to be published in this article.

Disclosure of conflict of interest

None.

Address correspondence to: Guang Chen, Department of Cardiothoracic Surgery, Zhuzou Central Hospital, No. 116 Changjiang South Road, Tianyuan District, Zhuzhou 412007, Hunan Province, China. Tel: +86-0731-28561316; E-mail: guangchen6353@163.com

References

[1] Siegel RL, Miller KD and Jemal A. Cancer statistics, 2019. CA Cancer J Clin 2019; 69: 7-34.
[2] Alvarado-Luna G and Morales-Espinosa D. Treatment for small cell lung cancer, where are we now?-A review. Transl Lung Cancer Res 2016; 5: 26-38.
[3] Herbst RS, Morgensztern D and Boshoff C. The biology and management of non-small cell lung cancer. Nature 2018; 553: 446-454.
[4] Zappa C and Mousa SA. Non-small cell lung cancer: current treatment and future advances. Transl Lung Cancer Res 2016; 5: 288-300.
[5] Koppenol WH, Bounds PL and Dang CV. Otto Warburg's contributions to current concepts of cancer metabolism. Nat Rev Cancer 2011; 11: 325-337.
[6] Warburg O. On the origin of cancer cells. Science 1956; 123: 309-314.
[7] Zuo Q, He J, Zhang S, Wang H, Jin G, Jin H, Cheng Z, Tao X, Yu C, Li B, Yang C, Wang S, Lv Y, Zhao F, Yao M, Cong W, Wang C and Qin W. PGC1alpha suppresses metastasis of HCC by inhibiting Warburg effect via PPARgamma-dependent WNT/beta-catenin/PDK1 axis. Hepatology 2020.
[8] Jing YY, Cai FF, Zhang L, Han J, Yang L, Tang F, Li YB, Chang JF, Sun F, Yang XM, Sun FL and Chen S. Epigenetic regulation of the Warburg effect by H2B monoubiquitination. Cell Death Differ 2020; 27: 1660-1676.
[9] Li J, He Y, Tan Z, Lu J, Li L, Song X, Shi F, Xie L, You S, Luo X, Li N, Li Y, Liu X, Tang M, Weng X, Yi W, Fan J, Zhou J, Qiang G, Qiu S, Wu W, Bode AM and Cao Y. Wild-type IDH2 promotes the Warburg effect and tumor growth through HIF1alpha in lung cancer. Theranostics 2018; 8: 4050-4061.

[10] Fraile JM, Quesada V, Rodríguez D, Freije JM and López-Otín C. Deubiquitinases in cancer: new functions and therapeutic options. Oncogene 2012; 31: 2373-2388.
[11] Shi J, Liu Y, Xu X, Zhang W, Yu T, Jia J and Liu C. Deubiquitinase USP47/UBP64E regulates beta-catenin ubiquitination and degradation and plays a positive role in Wnt signaling. Mol Cell Biol 2015; 35: 3301-3311.
[12] Silvestrini VC, Thome CH, Albuquerque D, de Souza Palma C, Ferreira GA, Lanfredi GP, Masson AP, Delsin LEA, Ferreira FU, de Souza FC, de Godoy LMF, Aquino A, Carrilho E, Panepucci RA, Covas DT and FaçaVM. Proteomics analysis reveals the role of ubiquitin specific protease (USP47) in epithelial to mesenchymal transition (EMT) induced by TGFbeta2 in breast cells. J Proteomics 2020; 219: 103734.
[13] Pan B, Yang Y, Li J, Wang Y, Fang C, Yu FX and Xu Y. USP47-mediated deubiquitination and stabilization of YAP contributes to the progression of colorectal cancer. Protein Cell 2020; 11: 138-143.
[14] Davudian S, Mansoori B, Shajari N, Mohammadi A and Baradaran B. BACH1, the master regulator gene: a novel candidate target for cancer therapy. Gene 2016; 588: 30-37.
[15] Hu Y, Liu Q, Zhang M, Yan Y, Yu H and Ge L. MicroRNA-362-3p attenuates motor deficit following spinal cord injury via targeting paired box gene 2. J Integr Neurosci 2019; 18: 57-64.
[16] Kastenmayer RJ, Moore RM, Bright AL, Torres-Cruz R and Elkins WR. Select agent and toxin regulations: beyond the eighth edition of the guide for the care and use of laboratory animals. J Am Assoc Lab Anim Sci 2012; 51: 333-338.
[17] Wiel C, Le Gal K, Ibrahim MX, Jahangir CA, Kashif M, Yao H, Ziegler DV, Xu X, Ghosh T, Mondal T, Kanduri C, Lindahl P, Sayin VI and Bergo MO. BACH1 stabilization by antioxidants stimulates lung cancer metastasis. Cell 2019; 178: 330-345, e322.
[18] Yang F, Xu J, Li H, Tan M, Xiong X and Sun Y. FBXW2 suppresses migration and invasion of lung cancer cells via promoting beta-catenin ubiquitylation and degradation. Nat Commun 2019; 10: 1382.
[19] Cai J, Li M, Wang X, Li L, Li Q, Hou Z, Jia H and Liu S. USP37 promotes lung cancer cell migration by stabilizing snail protein via deubiquitination. Front Genet 2019; 10: 1324.
[20] Yang R, Liu N, Chen L, Jiang Y, Shi Y, Mao C, Liu Y, Wang M, Lai W, Tang H, Gao M, Xiao D, Wang X, Zhou H, Tang CE, Liu W, Yu F, Cao Y, Yan Q, Liu S and Tao Y. GIAT4RA functions as a tumor suppressor in non-small cell lung cancer by counteracting Uchl3-mediated deubiquitination of LSH. Oncogene 2019; 38: 7133-7145.
[21] Yan S, Yue Y, Wang J, Li W, Sun M, Gu C and Zeng L. LINC00668 promotes tumorigenesis and progression through sponging miR-188-5p and regulating USP47 in colorectal cancer. Eur J Pharmacol 2019; 858: 172464.
[22] Hu L, Kolibaba H, Zhang S, Cao M, Niu H, Mei H, Hao Y, Xu Y and Yin Q. MicroRNA-204-5p inhibits ovarian cancer cell proliferation by down-regulating USP47. Cell Transplant 2019; 28 Suppl: 51S-58S.
[23] Zhang B, Yin Y, Hu Y, Zhang J, Bian Z, Song M, Hua D and Huang Z. MicroRNA-204-5p inhibits gastric cancer cell proliferation by downregulating USP47 and RAB22A. Med Oncol 2015; 32: 331.
[24] Liang CY, Li ZY, Gan TQ, Fang YY, Gan BL, Chen WJ, Dang YW, Shi K, Feng ZB and Chen G. Downregulation of hsa-microRNA-204-5p and identification of its potential regulatory network in non-small cell lung cancer: RT-qPCR, bioinformatic- and meta-analyses. Respir Res 2020; 21: 60.
[25] Lignitto L, LeBoeuf SE, Homer H, Jiang S, Askenazi M, Karakousi TR, Pass HI, Bhutkar AJ, Tsirigos A, Ueberheide B, Sayin VI, Papagiannakopoulos T and Pagano M. Nrf2 activation promotes lung cancer metastasis by inhibiting the degradation of Bach1. Cell 2019; 178: 316-329, e318.
[26] Naghavi L, Schwalbe M, Ghanem A and Naumann M. Deubiquitinylase USP47 promotes RelA phosphorylation and survival in gastric cancer cells. Biomedicines 2018; 6: 62.
[27] Yu L, Dong L, Wang Y, Liu L, Long H, Li H, Li J, Yang X, Liu Z, Duan G, Dai X and Lin Z. Reversible regulation of SATB1 ubiquitination by USP47 and SMURF2 mediates colon cancer cell proliferation and tumor progression. Cancer Lett 2019; 448: 40-51.
[28] Fan Q, Wang Q, Cai R, Yuan H and Xu M. The ubiquitin system: orchestrating cellular signals in non-small-cell lung cancer. Cell Mol Biol Lett 2020; 25: 1.
[29] Liu J, Shaik S, Dai X, Wu Q, Zhou X, Wang Z and Wei W. Targeting the ubiquitin pathway for cancer treatment. Biochim Biophys Acta 2015; 1855: 50-60.
[30] Kapuria V, Peterson LF, Fang D, Bornmann WG, Talpaz M and Donato NJ. Deubiquitinase inhibition by small-molecule WP1130 triggers aggresome formation and tumor cell apoptosis. Cancer Res 2010; 70: 9265-9276.
[31] Fu P, Du F, Liu Y, Yao M, Zhang S, Zheng X and Zheng S. WP1130 increases cisplatin sensitivity through inhibition of usp9x in estrogen receptor-negative breast cancer cells. Am J Transl Res 2017; 9: 1783-1791.
[32] Yuan BZ, Chapman J and Reynolds SH. Proteasome inhibitors induce apoptosis in human

lung cancer cells through a positive feedback mechanism and the subsequent Mcl-1 protein cleavage. Oncogene 2009; 28: 3775-3786.
[33] Lynch TJ, Fenton D, Hirsh V, Bodkin D, Middleman EL, Chiappori A, Halmos B, Favis R, Liu H, Trepicchio WL, Eton O and Shepherd FA. A randomized phase 2 study of erlotinib alone and in combination with bortezomib in previously treated advanced non-small cell lung cancer. J Thorac Oncol 2009; 4: 1002-1009.

Table S1. The primers for qRT-PCR assay

Primer Name	Primer Sequence (5'-3')
β-actin RT primer	random primer
β-actin Reverse primer	TGATCTTCATTGTGCTGGGTG
β-actin Forward primer	ACATCCGCAAAGACCTGTAC
USP47 RT primer	random primer
USP47 Reverse primer	AACCACAGATGTTACAAGGAGC
USP47 Forward primer	GGCGGAAGATCACCACGT
BACH1 RT primer	random primer
BACH1 Reverse primer	GGTTCTGGGCTCTCACTAATC
BACH1 Forward primer	AGGCTTCTGGAGTGACATTTG
Hk2 RT primer	random primer
Hk2 Reverse primer	ACATCACATTTCGGAGCCAG
Hk2 Forward primer	GGTGGACAGGATACGAGAAAAC
Gapdh RT primer	random primer
Gapdh Reverse primer	AAATGAGCCCCAGCCTTC
Gapdh Forward primer	AATCCCATCACCATCTTCCAG

Table S2. Antibodies used in this study

Antibody name	Corporation name	Catalog	Source	Poly/ monoclonal	Dilution ratio (WB)	Dilution ratio (IF/IHC)	Concentrations
USP47	Thermo Fisher Scientific	PA5-56103	rabbit	polyclonal	1:2000	1:50	1 mg/mL
	Thermo Fisher Scientific	37-0900	mouse	monoclonal	/	1:50	1 mg/mL
Ki67	Cell Signaling Technology	9449	mouse	monoclonal	1:1000	1:100	200 μg/mL
BACH1	Thermo Fisher Scientific	14018-1-AP	rabbit	polyclonal	1:2000	1:50	1 mg/mL
Poly-ub	Cell Signaling Technology	43126	rabbit	monoclonal	1:1000	/	200 μg/mL
Hk2	Cell Signaling Technology	2867	rabbit	monoclonal	1:1000	/	200 μg/mL
Gapdh	Cell Signaling Technology	5174	rabbit	monoclonal	1:1000	/	200 μg/mL
β-actin	Cell Signaling Technology	3700	mouse	monoclonal	1:1000	1:100	200 μg/mL
Goat anti-rabbit IgG	Thermo Fisher Scientific	31466	goat	monoclonal	1:2000	/	1 mg/mL
Goat anti-mouse IgG	Thermo Fisher Scientific	31431	goat	monoclonal	1:2000	/	1 mg/mL

Table S3. The sequences for shRNAs

shRNA Name	Sequence (5'-3')
BACH1	CACCGGACCAGAGGGATCTAGAAACCGAAGTTTCTAGATCCCTCTGGTCC
USP47	CACCGCTACATAAATGGAACCTTCGAAAAGGTTCCATTTATGTAGC

Table S4. The primers for plasmid constructs

Primer Name	Primer Sequence (5'-3')
BACH1 Reverse primer	CGGGTCGACTCTAGAGGTACCTTACTCATCAGTAGTACATTTATCAGTCATCT
BACH1 Forward primer	CGAGAATTCACGCGTGGTACCATGTCTCTGAGTGAGAACTCGGTTT

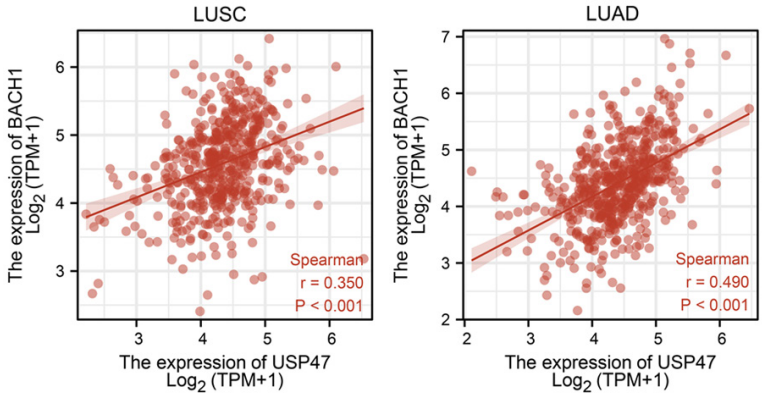

Figure S1. TCGA data analyses show that USP47 expression positively correlates with BACH1 expression.

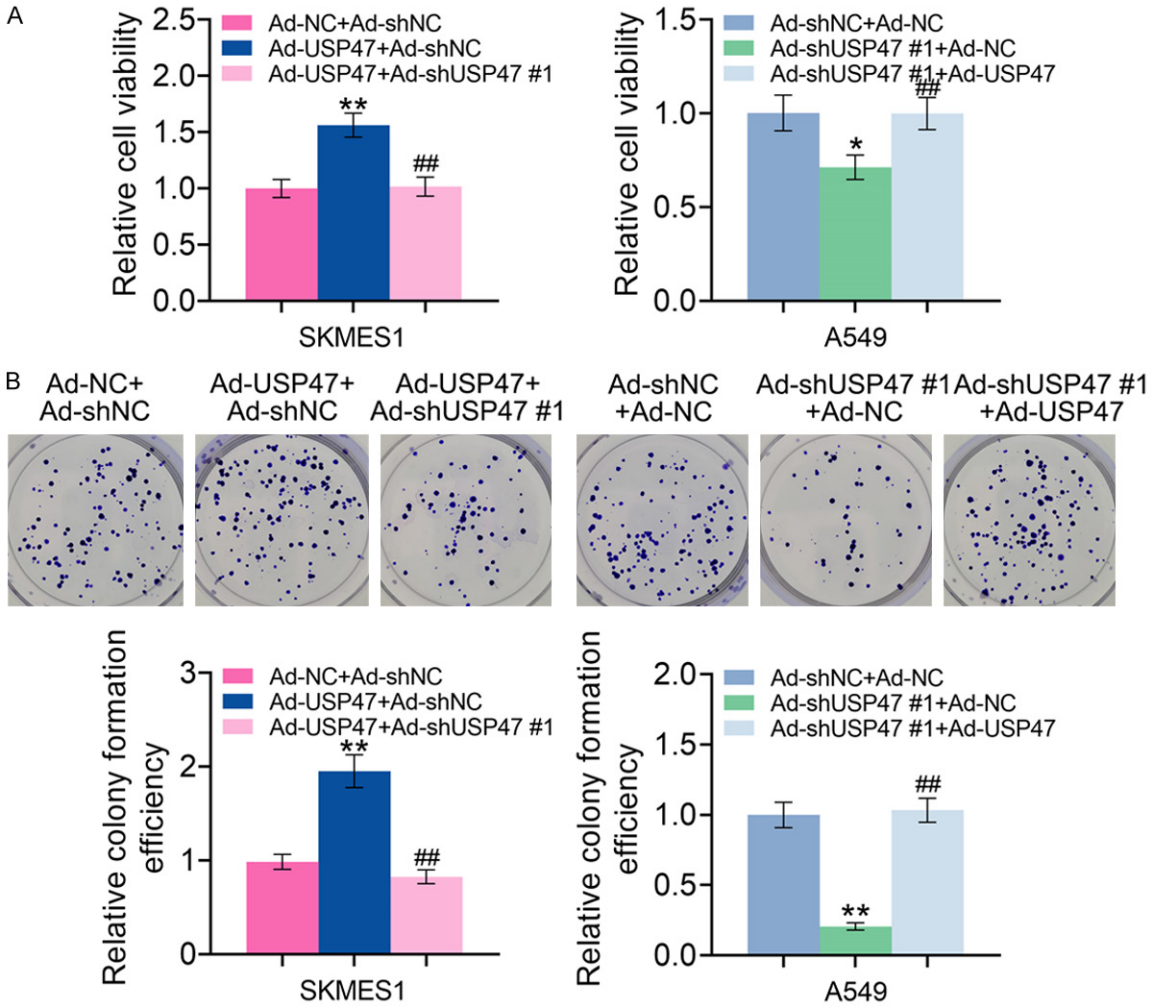

Figure S2. Suppression of USP47 in USP47 overexpression SKMES1 cells or overexpression of USP47 in USP47 depletion A549 cells could rescue cell viability and colony formation. (A) Relative cell viability and (B) Colony formation analysis of USP47 overexpression SKMES1 cells (Ad-USP47+Ad-shNC), suppression of USP47 in USP47 overexpression SKMES1 cells (Ad-USP47+Ad-shUSP47 #1) and the control cells (Ad-NC+Ad-shNC). And USP47 depletion A549 cells (Ad-shUSP47 #1+Ad-NC), overexpression of USP47 in USP47 depletion A549 cells (Ad-shUSP47 #1+Ad-USP47) and the control cells (Ad-shNC+Ad-NC). Measurements of the cell viability were obtained using a CCK-8 kit. Relative colony formation efficiency was quantified.

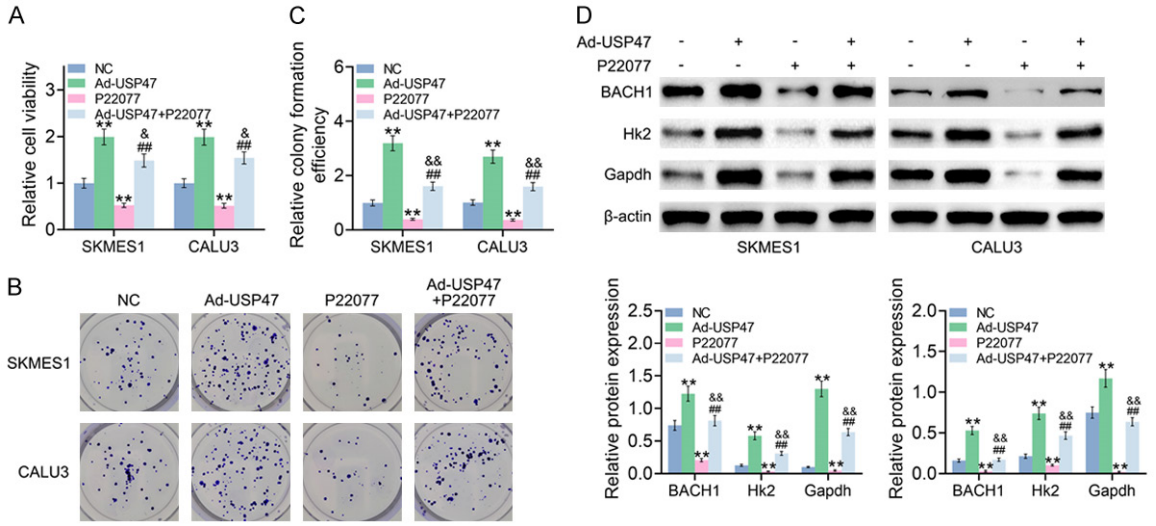

Figure S3. USP47 inhibitor P22077 suppress cell viability, colony formation and protein levels of BACH1, Hk2 and Gapdh. (A) Relative cell viability and (B) Colony formation analysis of USP47 overexpression SKMES1 and CALU3 cells (Ad-USP47), cells with P22077 treatment (P22077), USP47 overexpression cells with P22077 treatment (Ad-USP47+P22077) and the control cells (NC). Measurements of the cell viability were obtained using a CCK-8 kit. (C) Relative colony formation efficiency was quantified. (D) Relative BACH1, Hk2 and Gapdh protein expression levels in SKMES1 and CALU3 cells (Ad-USP47), cells with P22077 treatment (P22077), USP47 overexpression cells with P22077 treatment (Ad-USP47+P22077) and the control cells (NC). Bands were quantified and shown in histogram.

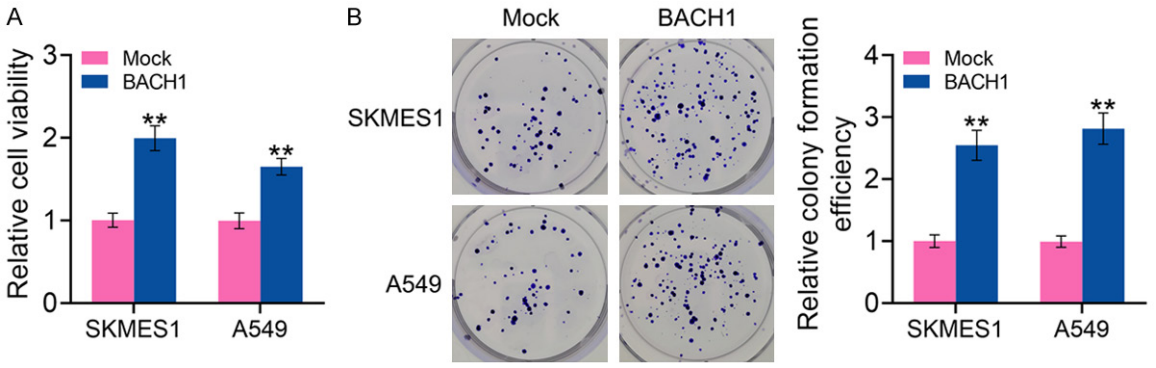

Figure S4. BACH1 overexpression promotes cell viability and colony formation. A. Relative cell viability of SKMES1 and A549 cells stably overexpressing BACH1 (BACH1) and the mock cells (Mock). Measurements of the cell viability were obtained using a CCK-8 kit. B. Colony formation analysis of SKMES1 and A549 cells stably overexpressing BACH1 (BACH1) and the mock cells (Mock). Relative colony formation efficiency was quantified.

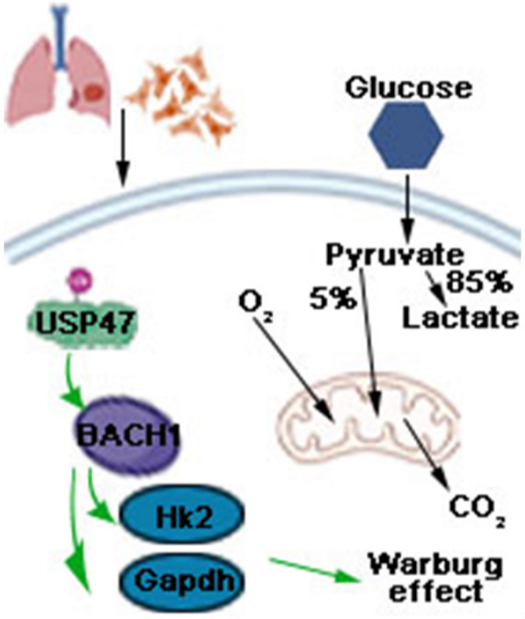

Figure S5. Mechanism diagram. During NSCLC development, overexpressed USP47 caused the deubiquitination of BACH1 and the downstream transcriptional regulation of hexokinase 2 (Hk2) and glyceraldehyde-phosphate dehydrogenase (Gapdh). Subsequently, the Warburg effect was promoted, which ultimately facilitated the tumor development. Targeting USP47/BACH1 axis might offer a new manner for NSCLC treatment.